Biosurface and Biotribology

WILEY

The Institution of Engineering and Technology

ORIGINAL RESEARCH OPEN ACCESS

Multifunctional Coating Based on Hyaluronic Acid Loaded With a Traditional Chinese Medicine Ingredient, Ophiopogon Saponin D, for Potential Application of Cardiovascular Stents

Jingan Li[1] | Kun Zhang[2] | Xiaojing Sun[1] | Zhongna Zhang[1] | Xiao Luo[3] | Shaokang Guan[1]

[1]School of Material Science and Engineering & Henan Province Key Laboratory of Advanced Light Alloys & Key Laboratory of Materials Processing and Mold Technology (Ministry of Education), Zhengzhou University, Zhengzhou, China | [2]School of Life Science, Zhengzhou University, Zhengzhou, China | [3]School of Medicine, University of Electronic Science and Technology of China, Chengdu, China

Correspondence: Jingan Li (lijingan@zzu.edu.cn) | Xiao Luo (luoxiao@uestc.edu.cn) | Shaokang Guan (skguan@zzu.edu.cn)

Received: 18 November 2025 | **Revised:** 25 January 2026 | **Accepted:** 8 February 2026

Keywords: biocompatibility | biointerface | biomaterials | cardiovascular device | coatings

ABSTRACT

Cardiovascular disease (CVD) is regarded as the leading cause of morbidity and mortality worldwide within recent decades. Stent intervention is one of the main methods for treating CVD due to its advantages of minimal trauma, fast recovery and fewer complications. However, the main function of existing drug-eluting stents is anti-hyperplasia, and their re-endothelialisation function is still insufficient and needs to be strengthened. In this study, a novel coating containing traditional Chinese medicine ingredient, Ophiopogon Saponin D (OPH), is designed to enhance the re-endothelialisation function of stents: firstly, the dopamine (DA) and hexanediamine (HD) were co-polymerised to the bare metal stent, endowing rich-amino surface (PDA/HD) for conjugating functional molecules by chemical reaction; thereafter hyaluronic acid (HA) containing OPH were conjugated to the PDA/HD. Our data suggested that the OPH coating promoted surface re-endothelialisation not only by directly enhancing proliferation/migration and inhibiting apoptosis of endothelial cells, but also by regulating macrophages to M2 phenotype and smooth muscle cells to contractile phenotype. Our study may provide inspiration for designing more novel biomaterial coatings using traditional Chinese medicine ingredient.

1 | Introduction

Cardiovascular diseases (CVD) persist as the leading cause of mortality globally driven by increasing atherosclerosis and vascular occlusions linked to the 'four high' risk factors: hypertension, hyperlipidaemia, hyperglycemia and hyperuricemia. This underscores the urgent need for effective preventive and therapeutic strategies to address these underlying factors [1]. Severe blood vessel blockages are commonly addressed through stent intervention, which is widely regarded as an effective method for reopening vessels, restoring blood flow and treating CVD [2]. However, currently the main drug eluting stents used in clinical practice are loaded with rapamycin and its derivatives, which not only inhibit hyperplasia but also delay the process of endothelialisation potentially leading to late-stage hyperplasia and thrombus formation [3]. Therefore, surface endothelialisation is crucial for the long-term efficacy of vascular stents with factors such as inflammation and hyperplasia potentially delaying this vital process [4]. In previous studies, it was often believed that endothelial cells (ECs) adhesion, proliferation and migration as well as endothelial progenitor cells (EPCs) capture are important factors promoting

Jingan Li and Kun Zhang are co-first-authors.

surface endothelialisation [5, 6]. However, macrophages and smooth muscle cells (SMCs) reach the stent surface much earlier than ECs [7]. Recent studies have found that specific subtypes of macrophages (M2 type) and SMCs (contractile type) also contribute to surface endothelialisation [8, 9]. Our previous research also found that regulating the transition of macrophages to M2 type and SMCs to contractile type can construct ordered endothelial structures of macrophages-SMCs-ECs from near to far on the surface of implanted materials under physiological conditions [10, 11]. Therefore, controlling the phenotypic changes of macrophages and SMCs becomes an additional important means of accelerating endothelialisation.

Designing stent coatings is a key strategy to enhance the physicochemical properties and biocompatibility of stents, thereby improving their overall performance [12]. The commonly used technique for endowing stents with 'double-sided adhesive' function is to utilise the chelating effect of dopamine and copolymerise it with hexamethylene diamine (HD) on the surface to prepare polydopamine (PDA)/HD (PDA/HD) thin films to increase surface amine density [13]. Furthermore, a range of functional molecules, such as heparin, hyaluronic acid (HA) and chondroitin sulphate, can be grafted onto the stent surface using methods such as electrostatic interactions, hydrogen bonding, physical adsorption and chemical reactions to enhance its functionality [14–16]. These composite coatings significantly improved the anti-coagulation, anti-inflammation, anti-hyperplasia and pro-endothelialisation functions. Our previous study also reported an astaxanthin loaded HA coating, which was conjugated on the PDA deposited magnesium alloy surface and demonstrated stronger pro-endothlialisation and anti-hyperplasia functions compared with the rapamycin coated magnesium alloy [17]. The reason why HA is widely used in the field of vascular stent coating design is due to its good nonimmunogenicity and drug loading performance [18]. In recent years, we have been trying to load the active ingredients of traditional Chinese medicine into HA for stent coating design, because the 5000-year history of traditional Chinese medicine has endowed humanity with too many mysterious miracles.

Ophiopogon japonicus is a traditional authentic Chinese medicinal herb, first found in the 'Shennong Bencao Jing' and classified as a top-grade (non-toxic) herb. It was one of the earliest drugs used in ancient China to treat cardiovascular diseases. Modern research has found that the main component of traditional Chinese medicine Ophiopogon japonicus, Ophiopogon Saponin D (OPH), is crucial in the management of cardiovascular diseases [19]. Our previous study also discovered that OPH promoted ECs growth and inhibited ECs apoptosis [20]. However, The OPH as an element of vascular stent multifunctional coating has not been explored systematically.

In this study, we incorporated OPH into HA solutions at varying concentrations (2, 4 and 8 mg/mL) and subsequently conjugated the OPH-loaded HA onto a polydopamine/hydroxyapatite (PDA/HD) coated 316L stainless steel (316L SS) substrate. We comprehensively evaluate the coating's effects on platelet adhesion, ex vivo hemocompatibility, macrophage phenotype transformation, endothelial cell (EC) adhesion, proliferation, migration and apoptosis. Additionally, we explore the in vivo interactions between the coatings and various cell types. We posit that this HA coating, which incorporates traditional Chinese medicine ingredients, has potential applications beyond the surface modification of cardiovascular stents extending to a wider range of biomaterials and device-related fields.

2 | Materials and Methods

2.1 | Preparation of the PDA/HD-HA/OPH Coatings

The poly-dopamine/hexamethylenediamine (PDA/HD) coating was applied to 316LSS substrates (Φ10 mm, sourced from Baoji, China) using a previously described method [21]. The reaction solution was prepared by dissolving dopamine hydrochloride (1 mg/mL) and hexamethylenediamine (HD, 2.44 mg/mL) in a Tris buffer at pH 8.5. Following a 48-h deposition period, the samples were rinsed with deionised water. The as-deposited coatings were then tempered at 120°C for 1 h under a vacuum of 5×10^{-4} Pa. Traditional Chinese medicine ingredient, Ophiopogon Saponin D (OPH), was dissolved in 2 mg/mL of hyaluronic acid (HA, 1×10^5 Da, Bloom Biotechnology Ltd., China) with gradient concentration of 2, 4 and 8 mg/mL, respectively. The HA solutions, both with and without OPH, were preactivated for 15 min. This activating solution comprised 1 mg/mL N-(3-dimethylaminopropyl)-N′-ethylcarbodiimide, 0.24 mg/mL N-hydroxysuccinimide, and 9.76 mg/mL 2-(N-morpholino)ethanesulfonic acid hydrate [22]. All three components have a purity of ≥ 97.0% and were purchased from Sigma-Aldrich. Subsequently, the PDA/HD-coated 316L SS samples were immersed in the previously prepared HA and HA/OPH solutions. After a 12-h reaction period, the specimens were thoroughly washed with PBS (three times, 5 min each) followed by deionised water (three times, 5 min each) [17]. The samples were termed as OPH-0 (0 mg/mL OPH), OPH-2 (2 mg/mL OPH), OPH-4 (4 mg/mL OPH) and OPH-8 (8 mg/mL OPH), respectively. The preparation process of the PDA/HD-HA/OPH coatings was presented in Figure 1.

2.2 | Characterisation of Coatings

The amine density of PDA/HA coating was detected by the Acid Orange II (AO II) colourimetric method [23]. Surface chemical bonds and elemental compositions were characterised by Fourier transform infrared spectroscopy (FTIR, BRUKER OPTIK GmbH Tensor II, Germany) and X-ray photoelectron spectroscopy (XPS, Kratos AXIS Supra, Japan), respectively [24, 25]. The morphology and roughness were determined by scanning electron microscopy (SEM, Thermo Scientific Helios G4 CX, USA) and atomic force microscopy (AFM, Bruker Size ICON, Germany) [26, 27]. Water contact angles of the 316LSS, PDA/HD, OPH-0, OPH-2, OPH-4 and OPH-8 samples were measured to assess the hydrophilicity using a contact angle apparatus (DSA 100, Krüss, GmbH, Germany) [28].

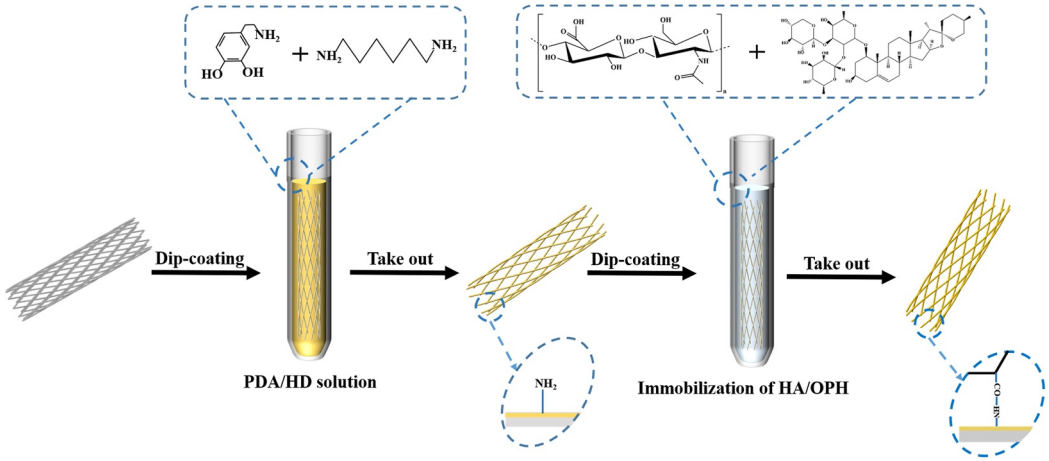

FIGURE 1 | The scheme of preparing PDA/HD-HA/OPH coatings on the 316L SS surface.

2.3 | Blood Compatibility

The blood compatibility was evaluated through platelet adhesion assays and ex vivo blood testing as detailed in our previous study [21].

2.4 | In Vitro Cytocompatibility

Human umbilical vein endothelial cells between third and fifth passages were utilised. The OPH-0, OPH-2, OPH-4, OPH-8, PDA/HD and 316LSS samples were placed in a 24-well culture plate. The cells at a concentration 5×10^4 cells/mL were seeded onto the samples and cultured for 1 and 3 days, respectively. The samples were stained with Rhodamine reagent (Sigma, USA) and 4′,6-diamidino-2-phenylindole (DAPI) and then examined using a fluorescence microscope (DMRX, Leica, Germany) to assess cellular morphology and distribution [29]. A Cell Counting Kit-8 (CCK-8) assay was employed to evaluate ECs attachment and proliferation [30]. The ECs apoptosis was evaluated by a typical AO/PI staining method, and the viability was also calculated [31]. To further evaluate the endothelialisation potential of the PDA/HD-HA/OPH coatings, a ECs migration experiment was conducted. Briefly, ECs were seeded at a density of 1×10^5 cells/mL onto one arm of L-shaped sample disks. After a 6-h incubation period, the samples were repositioned to allow cell migration to the opposite arm. Following a 24-h period, the cells were fixed and stained for F-actin to visualise the cytoskeletal structure. The samples were then examined using a fluorescence microscope [32].

To assess the anti-inflammatory properties of PDA/HD-HA/OPH coatings, an in vitro study was conducted wherein macrophages were cultured and subsequently analysed for cytokine secretion profiles. Specifically, the macrophages were seeded onto each sample at a concentration of 5×10^4 cells/mL and incubated at 37°C for durations of 3 and 5 days, respectively. To investigate the macrophage phenotype on each sample, fluorescence staining was conducted on the attached macrophages using CD32 antibody, which is specific for pro-inflammatory M1 macrophages, and CD206 antibody, specific for anti-inflammatory M2 macrophages. The number of cells on each sample was statistically counted from 15 randomly selected images [33]. The supernatant collected from macrophages cultured on the samples was used as the specimen. The release levels of tumour necrosis factor-alpha (TNF-α) and interleukin-10 (IL-10) were quantified using the respective assay kits following the manufacturer's instructions [34].

2.5 | In Vivo Tissue Response Evaluation

All procedures were conducted in accordance with the ethical guidelines for experimental animals as stipulated by the China Council on Animal Care and the Zhengzhou University animal use protocol (ZZUIRB2021-142).

2.5.1 | Aortic Implantation in Sprague-Dawley Rats

This experiment involved the implantation of bare 316L SS wires (Φ0.1 mm × 10 mm) and 316L SS wires coated with PDA/HD, OPH-0, OPH-2, OPH-4 and OPH-8 into the lumen of the abdominal aorta of Sprague-Dawley rats for a duration of 28 days. Then, 3 specimens were collected at each time point, and the aortas with implanted wires were retrieved [21]. They were rapidly frozen in liquid nitrogen and then cryo-sectioned for histological analysis. The cross sections were fixed in ethanol and subsequently stained with antibodies specific for endothelial cells (CD31, Sigma), smooth muscle cells (α-SMA and osteopontin (OPN), Sigma) and macrophages (CD32 and CD206, Sigma). Additionally, all nuclei were stained with DAPI (Sigma) [21].

2.5.2 | Iliac Artery Stent Implantation in New Zealand White Rabbits

Stent implantation in the Iliac Artery of New Zealand white rabbits for 28 days was performed as described by our previous study [21]. The morphology of the regenerated tissues covering the stents was examined using SEM to evaluate its tissue compatibility.

2.6 | Statistical Analysis

The data were statistically analysed using ANOVA beginning with a test for homogeneity of variances. Subsequently, post hoc comparisons were conducted using the LSD method. The results are presented as the mean ± standard deviation (SD). A probability value of $p < 0.05$ was considered indicative of a statistically significant difference. Data analysis was conducted using SPSS version 11.5 (Chicago, IL).

3 | Results and Discussion

Co-polymerisation of dopamine and hexamethylendiamine (HD) is generally considered to be an effective method to endow the surface higher amine density [35], and our results in Figure 2A showed PDA/HD samples presented higher amine density compared to bare 316L SS surface, which confirmed the successful deposition of the PDA/HD polymer. SEM images in Figure 2B showed PDA/HD, OPH-0, OPH-2, OPH-4 and OPH-8 samples displayed rougher surfaces compared with bare 316L SS sample. To further distinguish the surface morphology of the coating samples, roughness of each sample was scanned by AFM (Figure 2C): 316L SS showed its roughness of 3.23 ± 0.19 nm presenting a smooth surface that be well polished; PDA/HD, OPH-0, OPH-2, OPH-4 and OPH-8 samples showed rougher surfaces than 316L SS, which is consistent with the SEM result, wherein PDA/HD showed its roughness of 27.27 ± 4.51 nm, and OPH-0 showed its roughness of 47.57 ± 10.22 nm; the OPH loaded coatings (OPH-2, OPH-4 and OPH-8) presented rougher surface than the non-OPH surfaces, wherein OPH-2 showed its roughness of 62.13 ± 5.1 nm, OPH-4 showed its roughness of 70.9 ± 3.92 nm and OPH-8 showed its roughness of 82.8 ± 15.75 nm. As shown in Figure 2D, 316L SS sample possessed a hydrophilic surface with the water contact angle of 73.28 ± 1.88°; after PDA/HD deposition, the water contact angle decreased to 66.4 ± 0.34°; HA modification made the surface more hydrophilic (63.6 ± 1.47°), whereas OPH loading endowed the most hydrophilic surface, which may contribute to more protein adhesion and cell spreading.

To verify the successful conjugation of OPH-loaded HA onto the PDA/HD film, the surface chemical compositions of the PDA/HD film and the coatings with varying OPH concentrations (OPH-0, OPH-2, OPH-4, OPH-8) were analysed using FTIR and XPS. FTIR results in Figure 3A showed the wide blunt peaks appeared at the wavelength of 3100–3200 cm^{-1} in all samples, and these characteristic peaks may be derived from hydroxyl/phenolic hydroxyl (-OH) and amino ($-NH_2$) groups, which may be derived from dopamine and HA. Two small raised acromial peaks appeared at 2924 and 2853 cm^{-1} wavelengths, which may be due to the presence of methylene ($-CH_2-$). A small convex acromion appeared in the wavelength range of 700–900 cm^{-1}, and the appearance of this characteristic peak proved that the coating contained adjacent, intermediate and para substitutional functional groups of benzene ring originating from dopamine. Consequently, the appearance of these characteristic peaks confirmed the successful preparation of PDA/HD. At the same time, OPH series samples showed a small raised acromion

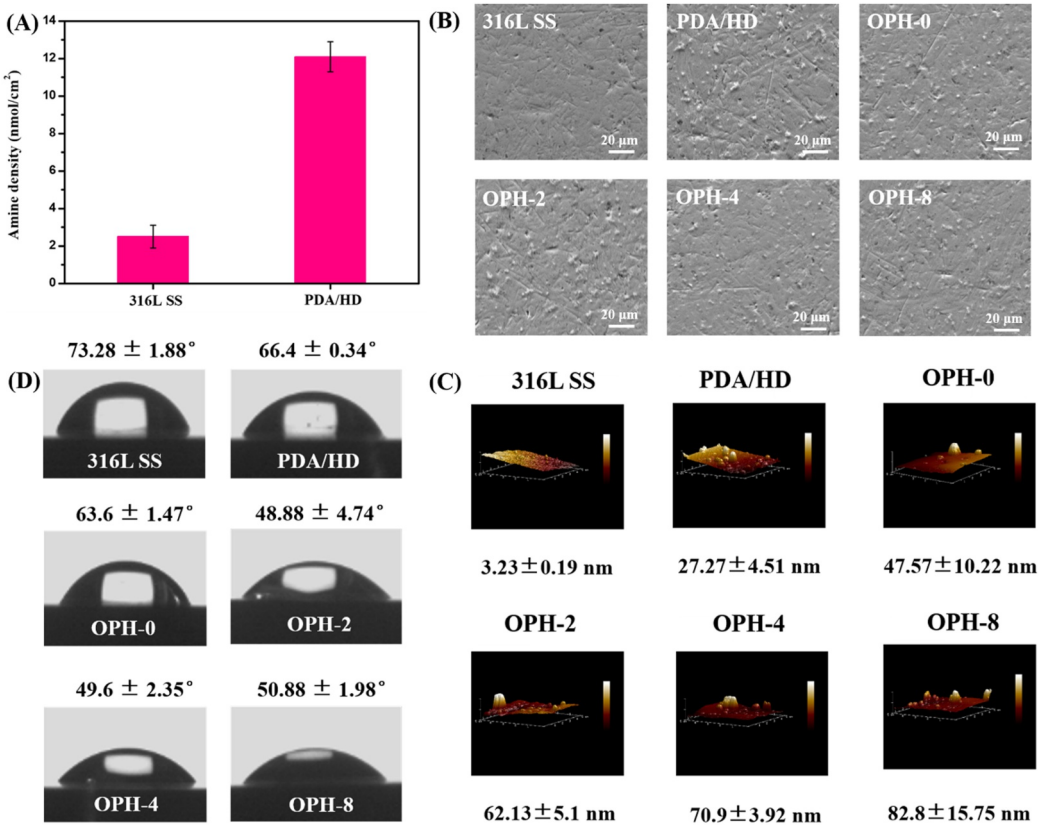

FIGURE 2 | (A) Surface amine concentration of 316LSS and PDA/HD samples (mean ± SD, $N = 3$); (B) SEM images (C) AFM images and (D) water contact angles of 316L SS, PDA/HD, OPH-0, OPH-2, OPH-4 and OPH-8 samples surfaces (mean ± SD, $N = 6$).

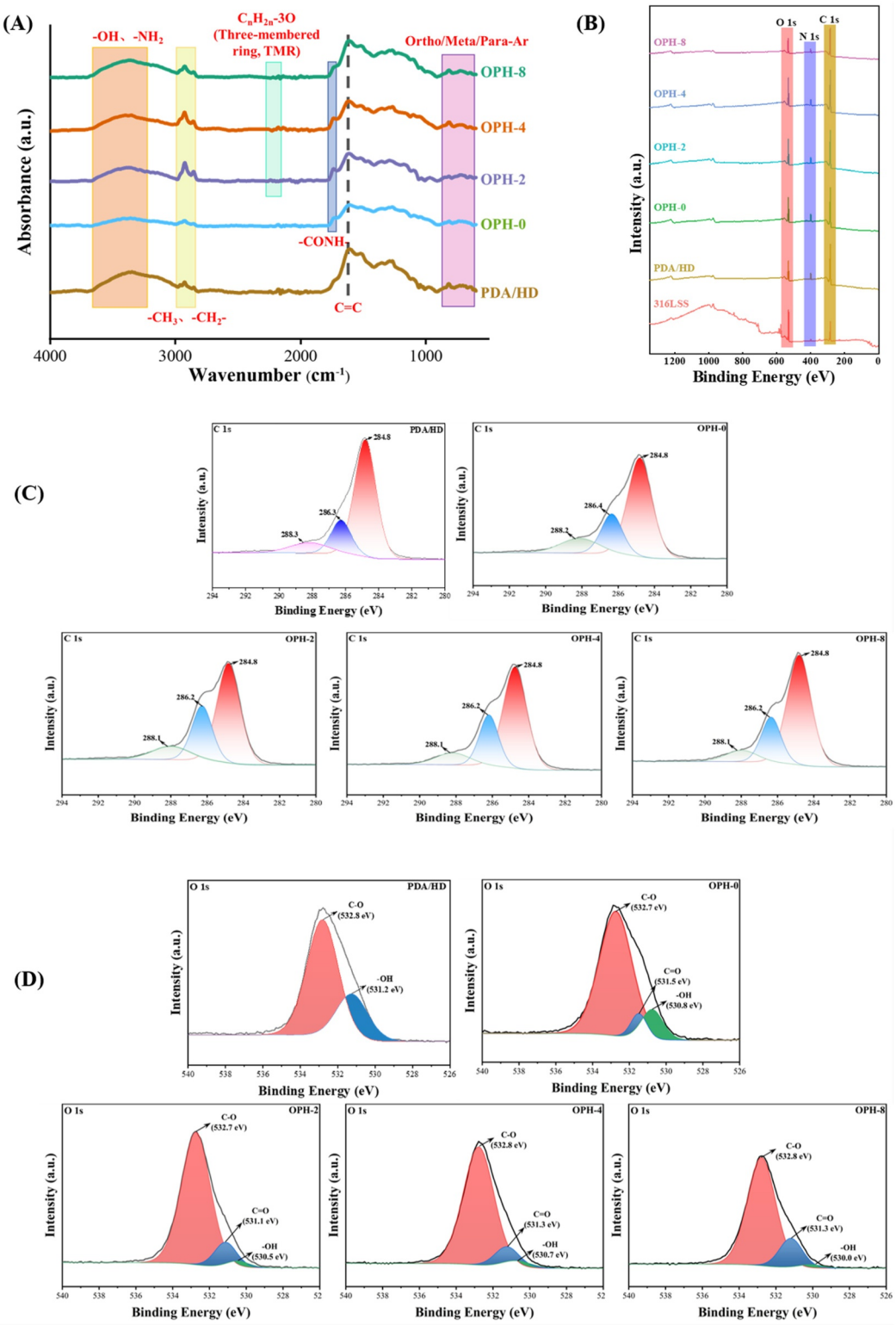

FIGURE 3 | (A) FTIR spectra, (B) XPS full spectrum, (C) comparison of the C1s and (D) the O 1s high-resolution spectra of the PDA/HD, OPH-0, OPH-2, OPH-4 and OPH-8.

at 2960 cm^{-1} wavelength, indicating that the sample may contain methyl (-CH_3). The emergence of a prominent peak at a wavelength of 1740 cm^{-1} indicated the presence of an amide bond (-CONH-) within the sample. This bond was formed through a dehydration condensation reaction between the amino group in PDA/HD and the carboxyl group in HA, thereby demonstrating the successful preparation of the OPH-0 coating. In addition, OPH-2, OPH-4 and OPH-8 samples showed two smaller bumps at 2180 and 2145 cm^{-1} wavelengths, indicating that the sample may contain terrains, which are derived from

saponins, and the presence of this functional group proves that OPH was successfully coated by HA and loaded onto the PDA/HD coating.

As observed in the XPS full spectrum (Figure 3B), distinct absorption peaks corresponding to C 1s, O 1s and N 1s were evident on the surface of each sample group. This finding confirms the presence of these three elements in all the samples. The high-resolution spectral diagram of C 1s is shown in Figure 3C. Based on the chemical state of the element, the C 1s peak (calibrated to 284.8 eV) is deconvoluted into distinct carbon peaks. For the PDA/HD samples, the C 1s peaks are categorised into C-C/C-H peaks at 284.8 eV, C-OH/C-N/C=N peaks at 286.3 eV and C=O peaks at 288.3 eV. These characteristic peaks primarily originated from the phenolic hydroxyl and amino groups of PDA/HD as well as the dopamine quinone formed through oxidation during the polymerisation of dopamine. For the OPH series samples, the C 1s peaks were deconvoluted into C-C/C-H peaks at 284.8 eV, C-O/C-O-C peaks at 286.2 eV and N-C=O peaks at 288.1 eV. The C-O/C-O-C peaks primarily originated from the ether bonds and hydroxyl groups present in HA. The N-C=O peak resulted from the formation of an amide bond, which occurred through the dehydration and condensation reaction between PDA/HD and HA. The high-resolution spectra of O 1s, depicted in Figure 3D, reveal the distinct oxygen-related chemical states in the samples. For the PDA/HD sample, the spectrum shows C-O peaks at 532.8 eV and -OH peaks at 531.2 eV both attributed to the phenolic hydroxyl groups of dopamine. In contrast, the OPH series samples exhibit not only the C-O and -OH peaks but also a pronounced C=O peak near 531 eV. This additional peak is primarily due to the presence of amide bonds formed during the reaction. These distinct peaks of carbon and oxygen correlate with the characteristic absorption peaks observed in infrared spectroscopy, confirming the successful preparation of the OPH composite coatings.

After stent implantation, platelets in the circulating blood flow may adherent on the materials' surface and trigger serious coagulation, which may lead to thrombogenesis and block the lumen of blood vessels [36]. Thus, investigating platelet adhesion is an important aspect for evaluating new coatings of stents. Figure 4 demonstrates that the OPH-0, OPH-2, OPH-4 and OPH-8 coatings resulted in reduced platelet adhesion compared to 316L SS. However, the drug-loaded HA coatings did not exhibit enhanced anti-platelet adhesion properties compared to the nondrug HA coatings, indicating that the HA itself, rather than the drug, was responsible for inhibiting platelet adhesion.

To further assess the hemocompatibility of each sample under dynamic blood flow conditions, an ex vivo experiment was conducted using New Zealand white rabbits. Figure 5A shows that OPH drug-loaded samples produced a wider lumen compared to 316L SS, PDA/HD and OPH-0 samples. This observation was corroborated by the evaluations of lumen loss rate and thrombus weight, which showed consistent results across these metrics (Figure 5B,C). Wherein OPH-2 and OPH-4 samples presented fewer whole blood composition compared with the other samples, which was observed from SEM images (Figure 5D).

Endothelial cells, as the primary component of the inner layer of blood vessels, play a crucial role in achieving long-term anticoagulation, anti-hyperplasia and anti-inflammatory effects on stent surfaces through rapid endothelialisation [37]. Figure 6 demonstrated that all coating samples enhanced ECs adhesion and proliferation compared to the bare 316L SS with OPH-4 showing the highest ECs presence. Consistent with these findings, the ECs migration experiment revealed that the OPH-4 sample facilitated greater ECs migration distances than other samples (Figure 7A). Further investigation into ECs apoptosis prevention, as shown in the living/dead staining images in Figure 7B and the survival rate calculations from 15 random images (Figure 7C), indicated that OPH-0, OPH-2 and OPH-4 exhibited superior ECs apoptosis prevention capabilities. All the results above indicated the OPH coatings possessed strong functions to promote surface endothelialisation.

After stent implantation, macrophages are the earliest batch of cells to reach the surface and play a major role in the inflammatory response [38]. It is worth noting that the surface of materials

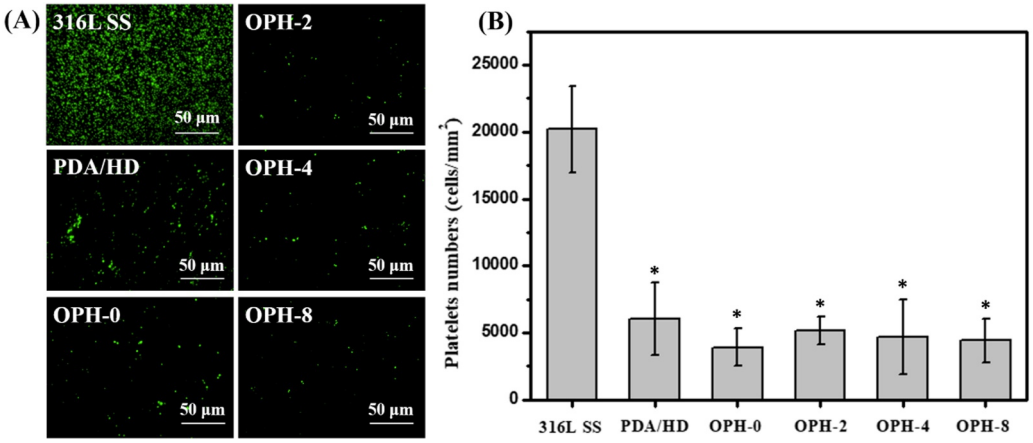

FIGURE 4 | (A) Fluorescence images of adherent platelets stained with rhodamine on the 316L SS, PDA/HD film, OPH-0, OPH-2, OPH-4 and OPH-8; (B) platelets numbers of the 16L SS, PDA/HD film, OPH-0, OPH-2, OPH-4 and OPH-8 samples (*$p < 0.05$, compared with 316L SS, mean ± SD, $n = 15$).

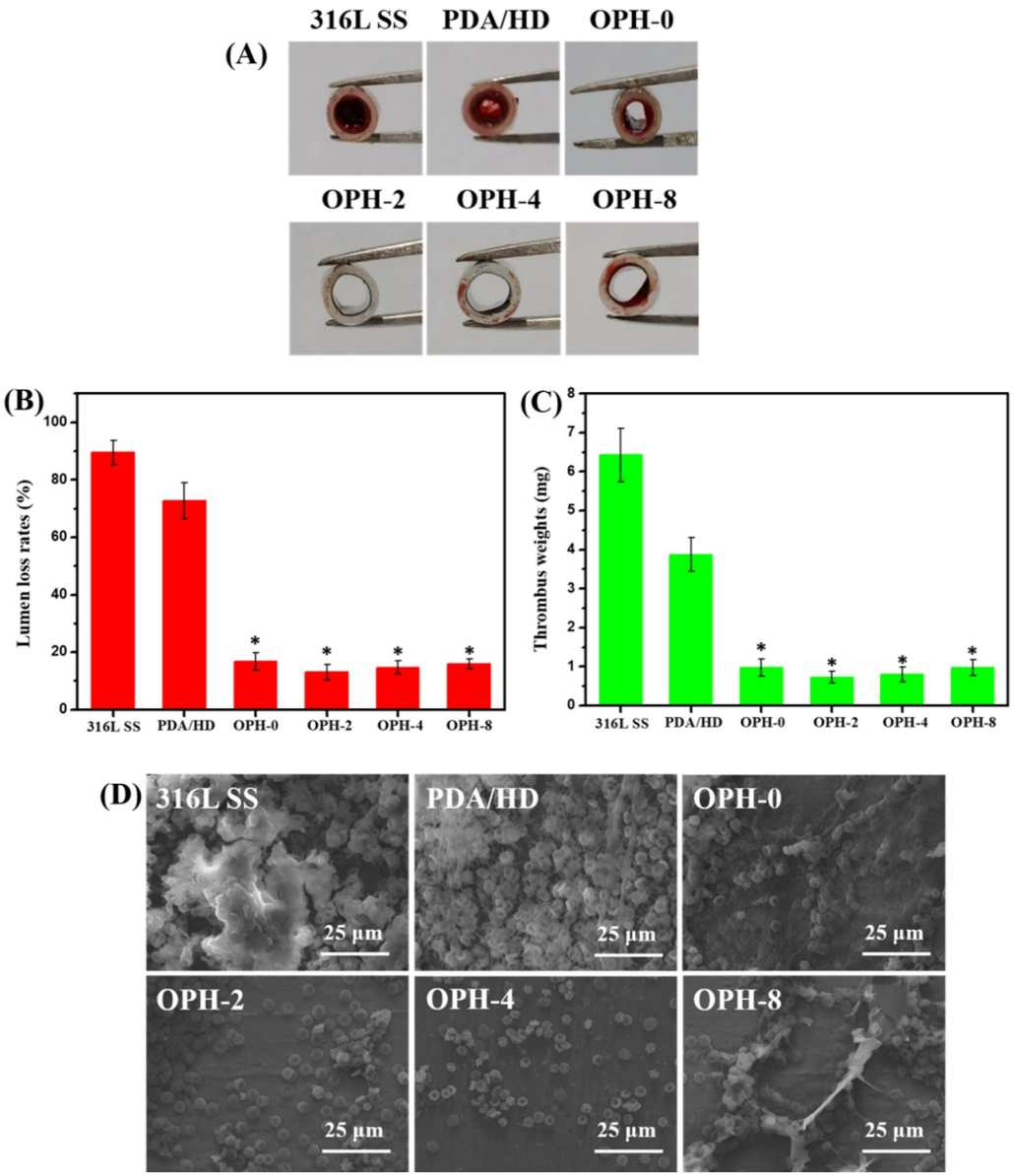

FIGURE 5 | Ex vivo experiment on New Zealand white rabbit: (A) cross-sectional and surface micrographs of cavities containing 316L SS, PDA/HD, OPH-0, OPH-2, OPH-4 and OPH-8 samples following experiment; (B) lumen loss rates and (C) thrombosis weight for each sample type (*$p < 0.05$, compared with 316L SS, mean ± SD, $n = 3$); (D) SEM images depicting the adherence of blood components on the surfaces of 316L SS, PDA/HD, OPH-0, OPH-2, OPH-4 and OPH-8.

can be regulated by designing coatings to regulate the phenotype of macrophages, and the phenotype of adhered macrophages further determines whether the surface delays or promotes endothelialisation [39]. The previous study proved that the pro-inflammatory M1 macrophages interference and delay surface endothelialisation whereas anti-inflammatory M2 macrophages promote endothelialisation [40]. CD32 and CD206 are typically used as specific markers for M1 and M2 macrophages, respectively [21, 41]. In our data (Figure 8A), the adherent macrophages on the composite coatings composed of HA presented higher CD206 expression (green colour) and lower CD32 expression (red colour), suggesting pro-M2 effect of the HA, which is consistent with the previous report [21]. The OPH loaded coatings showed higher CD206 expression (green colour) and lower CD32 expression compared to the single HA coating. This result indicated the traditional Chinese medicine ingredient, OPH, possessed strong function of regulating macrophages from M1 to M2 phenotype, which may endow the surface better ability of endothelialisation. The macrophage counting results indicated that the number of macrophages on the OPH-loaded coatings was significantly lower compared to other samples (Figure 8B). Additionally, macrophages on the OPH-loaded coatings released lower levels of the inflammatory factor TNF-α (Figure 8C) and higher levels of the anti-inflammatory factor IL-10 (Figure 8D). These findings further support the anti-inflammatory efficacy of the OPH-loaded coatings. Obviously, the function of coatings in

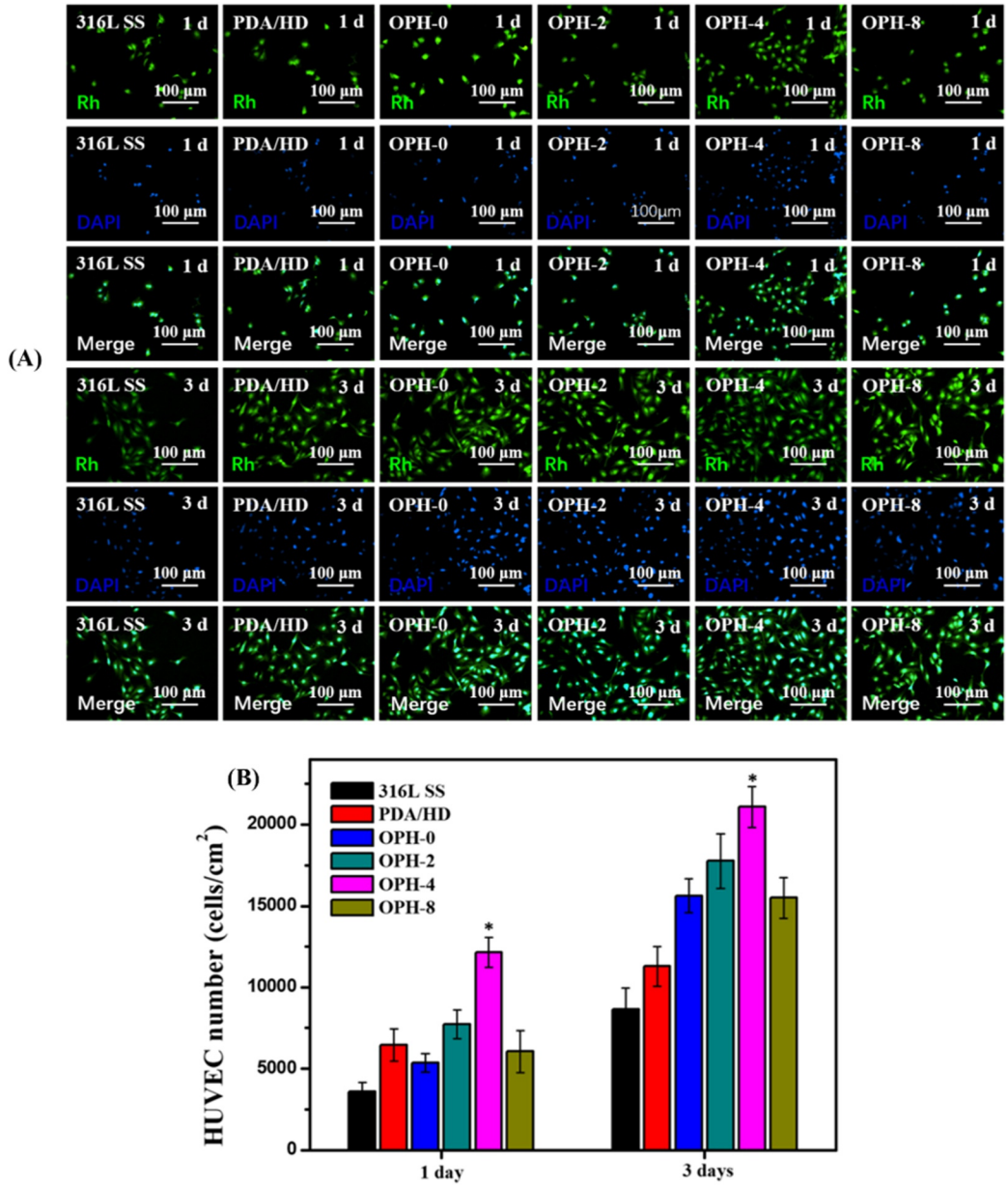

FIGURE 6 | (A) Fluorescence images of ECs culture on the 316L SS, PDA/HD, OPH-0, OPH-2, OPH-4 and OPH-8 surfaces for 1 and 3 days, respectively (Green colour: rhodamine; blue colour: DAPI); (B) amount of ECs on the 316L SS, PDA/HD, OPH-0, OPH-2, OPH-4 and OPH-8 surfaces after culture for 1 and 3 days, respectively (*$p < 0.05$, compared with all the other samples, mean ± SD, $n = 3$).

regulating macrophage factor release is correlated with the loading amount of OPH, and the more OPH loaded, the stronger the regulatory function.

As shown in Figure 9, the 316L SS wire coated with OPH-0, OPH-2, OPH-4, OPH-8, PDA/HD and the bare 316L SS were implanted to the abdominal aorta of Sprague-Dawley rats. After 28 days, the treated samples were stained with specific antibodies to observe their pro-endothelialisation, anti-inflammation and anti-hyperplasia properties. The in vivo data showed that OPH-2, OPH-4 and OPH-8 (Samples loaded with traditional Chinese medicine) presented better pro-endothelialisation properties: The green thin line stained by CD31 antibody indicated the endothelial layer, which distributed around the outermost layer of newly formed tissue located near the blood flow. Wherein, the endothelial layer of OPH-8 sample was too thick, which will further affect its function, for the reason that single layer endothelium has better function. Compared to OPH-4, the green lines in OPH-2 are too fragmented obviously due to incomplete coverage of endothelial cells. Therefore, OPH-4 has the best endothelialisation function in the drug loaded coating. In addition, in vivo results also showed that, unlike the results observed in endothelial cell culture in vitro [42] in the complex microenvironment of blood vessels, endothelial cells do not directly grow on implanted wires but on contractile SMCs (α-SMA positive expression), which presented red colour and located closely to the

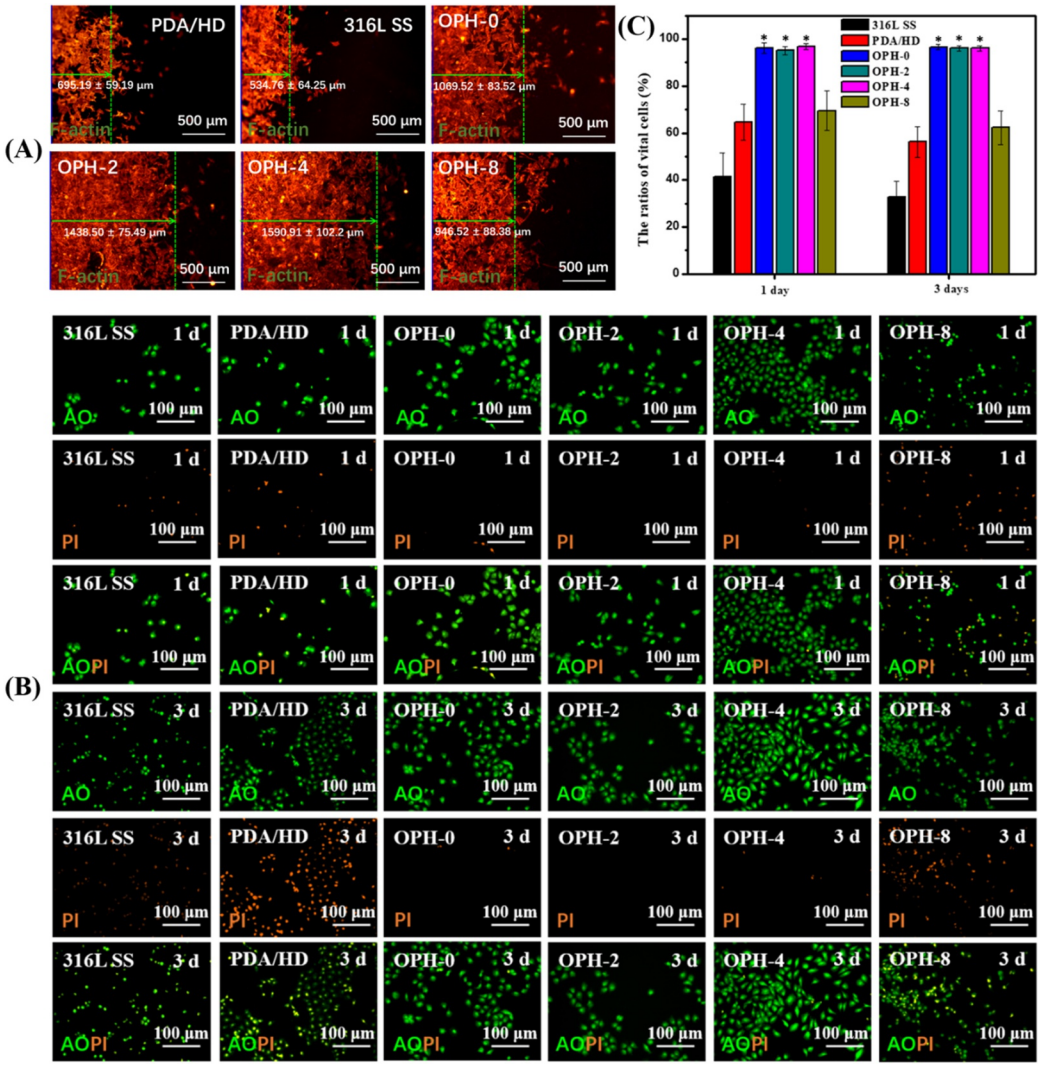

FIGURE 7 | (A) The migrated ECs on 316L SS, PDA/HD, OPH-0, OPH-2, OPH-4 and OPH-8 surfaces; (B) fluorescence staining of the ECs on 316L SS, PDA/HD, OPH-0, OPH-2, OPH-4 and OPH-8 surfaces after 1 and 3 days, respectively. The living ECs were stained by AO (green), and the dead or apoptotic ECs were stained with PI (orange); (C) statistical results of ECs survival rates on the 316L SS, PDA/HD, OPH-0, OPH-2, OPH-4 and OPH-8 surfaces after 1 and 3 days, respectively (*$p < 0.05$, compared with all the other samples, mean ± SD, $n = 15$).

single green line. In the OPH-4 group, the newly regenerated tissues exhibited higher expression of CD206 (a specific marker for M2 macrophages) and lower expression of CD32 (a specific marker for M1 macrophages) and OPN (a specific marker for synthetic smooth muscle cells, SMCs). These findings suggest that OPH-4 possesses enhanced anti-inflammatory and anti-hyperplasia properties. Furthermore, they imply that M2 macrophages and contractile SMCs actively and orderly contribute to the endothelialisation process playing a crucial role prior to the arrival of endothelial cells.

To further evaluate the effect of the optimised coating on the endothelialisation function of 316L SS stents, OPH-4 coated and bare 316L SS stents were implanted into the iliac artery of New Zealand white rabbits. SEM images in Figure 10 showed that the new regenerated tissue on bare 316L SS was incomplete and didn't completely cover the stent. In contrast, the endothelial tissue completely covered the OPH-4 coated stents indicating a superior pro-endothelialisation function.

4 | Conclusions

In this study, we incorporated the Traditional Chinese Medicine ingredient Ophiopogon Saponin D into hyaluronic acid at gradient concentrations (2, 4 and 8 mg/mL) to construct composite coatings on amine-rich surfaces (PDA/HD) with the aim of enhancing the multifunctionality of cardiovascular stents. The in vitro platelet adhesion and ex vivo blood tests demonstrated that these composite coatings significantly improved the blood compatibility of the substrate with OPH-2 (2 mg/mL) and OPH-4 (4 mg/mL) exhibiting superior performance. The HUVECs culture experiment demonstrated that all composite

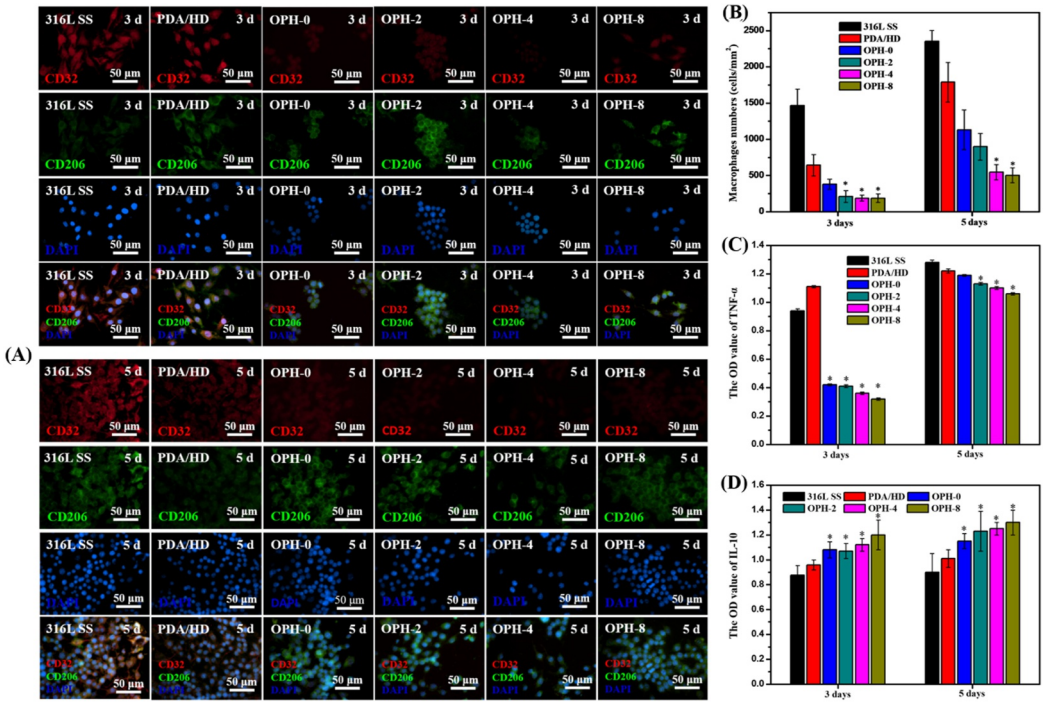

FIGURE 8 | (A) Immunofluorescence staining of macrophages on the 316L SS, PDA/HD, OPH-0, OPH-2, OPH-4 and OPH-8 surfaces for 3 and 5 days respectively (Green colour: cells expressed CD206; red colour: cells expressed CD32; blue colour: DAPI); (B) macrophages numbers of the 316L SS, PDA/HD, OPH-0, OPH-2, OPH-4 and OPH-8 surfaces, respectively (*$p < 0.05$, compared with all the other samples, mean ± SD, $n = 15$); (C) TNF-α and (D) IL-10 release from the macrophages (*$p < 0.05$, compared with all the other samples, mean ± SD, $n = 3$).

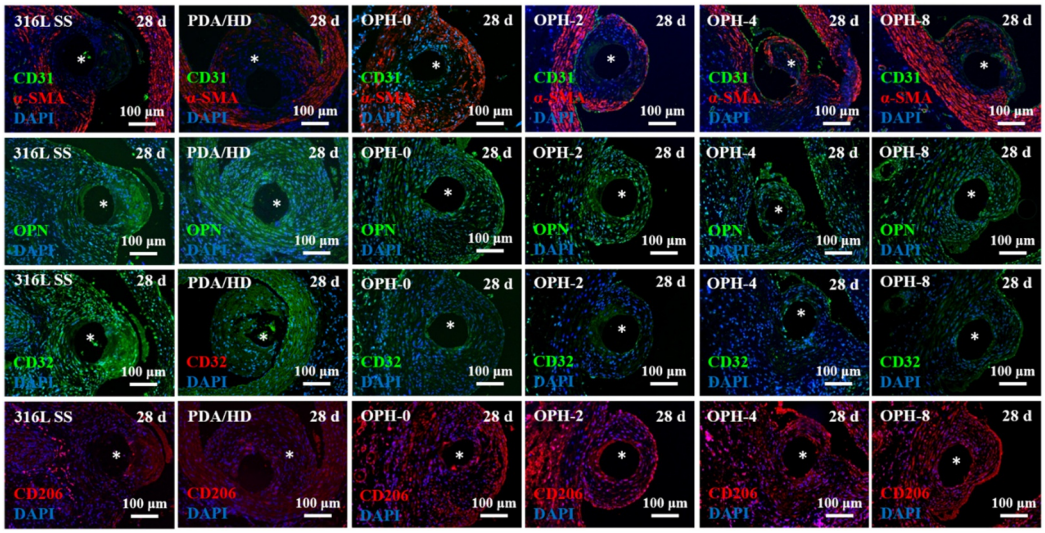

FIGURE 9 | Immunofluorescence staining for artery tissues around OPH-0, OPH-2, OPH-4, OPH-8, PDA/HD and 316L SS implants after 28 days (* indicates the location of each sample implanted).

coatings significantly inhibited endothelial cell apoptosis. Among them, the OPH-4 coating exhibited superior capabilities in promoting endothelial cell proliferation and migration. The in vitro macrophage phenotype-change assay indicated that all composite coatings significantly suppressed inflammation by reducing macrophage adhesion and cytokine release (TNF-α). Additionally, they facilitated the transition of adherent macrophages from the M1 to the M2 phenotype with the OPH-loaded coating demonstrating a particularly enhanced effect. Moreover, the in vivo wires and stents implantation experiments displayed that OPH-4 coatings had better abilities of anti-inflammation, anti-hyperplasia and improving surface endothelialisation. The endothelialisation process not only concluded endothelial cells adhesion/proliferation but also involved the phenotype regulation of macrophages (To M2) and SMCs (To contractile type). The endothelial cells didn't grow on the implants' surface directly but on the contractile SMCs tissue. These findings underscore the viability of utilising Traditional Chinese Medicine

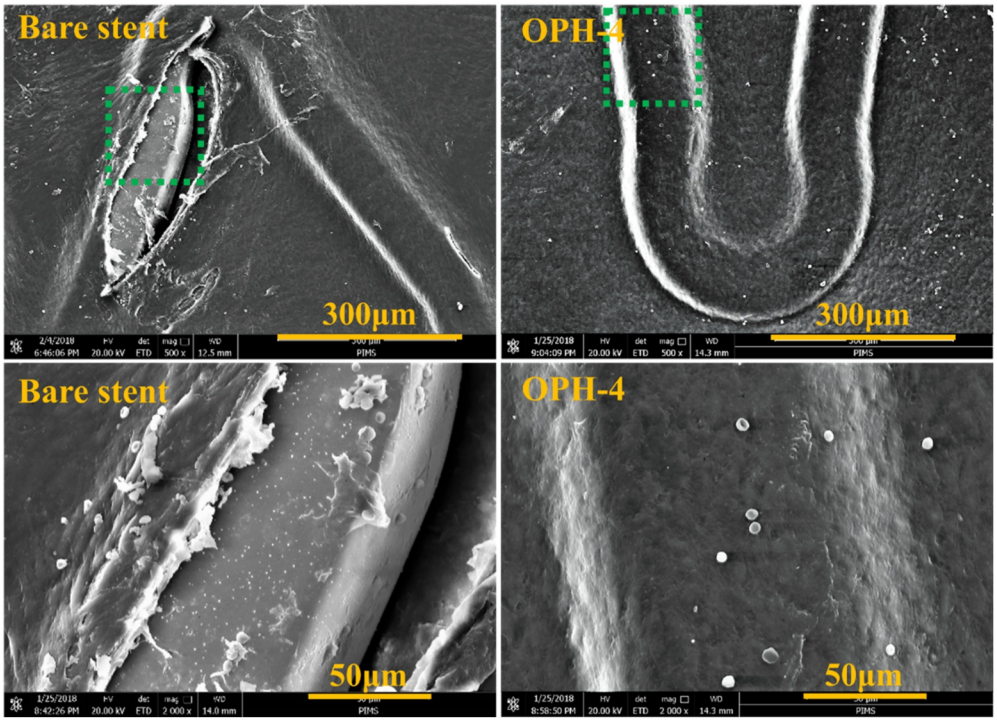

FIGURE 10 | Stent implantation in the iliac artery of New Zealand White Rabbits for 28 days: OPH-4 coated 316L SS stents versus bare 316L SS stents.

ingredient-loaded coatings for the surface modification of cardiovascular biomaterials presenting a gentler yet more efficacious alternative for potential applications.

Acknowledgements

The study was supported by the National Natural Science Foundation of China (U2004164) and Zhengzhou University Major Project Cultivation Special Project (125-32214076). We also express our gratitude to Bloomage Biotechnology Corporation Limited for supplying hyaluronic acid and providing technical support.

Conflicts of Interest

The authors declare no conflicts of interest.

Data Availability Statement

The data that support the findings of this study are available on request from the corresponding author.

References

1. Z. Xue, X. Sun, H. Li, et al., "Composite Coatings of S-HA Nanoparticles and Schiff Base on ZE21B Alloy for Stronger Corrosion Resistance and Biological Performance," *Journal of Magnesium and Alloys* 12, no. 11 (2024): 4547–4560, https://doi.org/10.1016/j.jma.2023.11.009.

2. K. Yahagi, F. D. Kolodgie, F. Otsuka, et al., "Pathophysiology of Native Coronary, Vein Graft, and In-Stent Atherosclerosis," *Nature Reviews Cardiology* 13, no. 2 (2016): 79–98, https://doi.org/10.1038/nrcardio.2015.164.

3. D. A. Zidar, "Newer-Generation Drug-Eluting Stents: Heal Thyself," *Science Translational Medicine* 5, no. 211 (2013): 211ec190, https://doi.org/10.1126/scitranslmed.3007981.

4. R. Wang, J. Lu, J. Yin, et al., "A TEMPOL and Rapamycin Loaded Nanofiber-Covered Stent Favors Endothelialization and Mitigates Neointimal Hyperplasia and Local Inflammation," *Bioactive Materials* 19 (2023): 666–677, https://doi.org/10.1016/j.bioactmat.2022.04.033.

5. P. Tong, L. Chen, X. Sun, et al., "Surface Modification of Biodegradable Magnesium Alloy With Poly (L-Lactic Acid) and Sulfonated Hyaluronic Acid Nanoparticles for Cardiovascular Application," *International Journal of Biological Macromolecules* 237 (2023): 124191, https://doi.org/10.1016/j.ijbiomac.2023.124191.

6. N. Werner, S. Kosiol, T. Schiegl, et al., "Circulating Endothelial Progenitor Cells and Cardiovascular Outcomes," *New England Journal of Medicine* 353, no. 10 (2005): 999–1007, https://doi.org/10.1056/nejmoa043814.

7. G. Li, P. Yang, X. Guo, N. Huang, and R. Shen, "An in Vitro Evaluation of Inflammation Response of Titanium Functionalized With Heparin/Fibronectin Complex," *Cytokine* 56, no. 2 (2011): 208–217, https://doi.org/10.1016/j.cyto.2011.06.020.

8. H. Wan, Y. Li, Y. Qin, et al., "Polyphenol-Mediated Sandwich-Like Coating Promotes Endothelialization and Vascular Healing," *Biomaterials* 302 (2023): 122346, https://doi.org/10.1016/j.biomaterials.2023.122346.

9. D. Tang, S. Chen, D. Hou, et al., "Regulation of Macrophage Polarization and Promotion of Endothelialization by NO Generating and PEG-YIGSR Modified Vascular Graft," *Materials Science and Engineering: C* 84 (2018): 1–11, https://doi.org/10.1016/j.msec.2017.11.005.

10. P. Shi, C. Lou, J. Fang, L. Zhang, W. Wang, and J. Li, "Tissue-Engineered Balloonfish Stomach Vascular Patches Coated With 4-Octyl Itaconate Inhibit Neointimal Hyperplasia," *Materials Today Communications* 43 (2025): 111746, https://doi.org/10.1016/j.mtcomm.2025.111746.

11. C. Zhang, S. Wei, L. Zhang, et al., "Silver Ion Decreases Foreign Body Reaction and Venous Neointimal Hyperplasia Through the Inhibition of Interleukin-33 Expression," *Journal of Vascular Research* 61, no. 2 (2024): 89–98, https://doi.org/10.1159/000536003.

12. X. Duan, Y. Yang, T. Zhang, B. Zhu, G. Wei, and H. Li, "Research Progress of Metal Biomaterials With Potential Applications as Cardiovascular Stents and Their Surface Treatment Methods to Improve Biocompatibility," *Heliyon* 10, no. 4 (2024): e25515, https://doi.org/10.1016/j.heliyon.2024.e25515.

13. Z. Du, F. Qiao, L. Tong, et al., "Mimicking Mytilus Edulis Foot Protein: A Versatile Strategy for Robust Biomedical Coatings," *Innovation* 5, no. 5 (2024): 100671, https://doi.org/10.1016/j.xinn.2024.100671.

14. L. Xu, C. He, S. Yang, et al., "Phase-Transited Lysozyme Nanofilm With Co-Immobilized Copper Ion and Heparin as Cardiovascular Stent Multifunctional Coating," *Colloids and Surfaces B: Biointerfaces* 230 (2023): 113530, https://doi.org/10.1016/j.colsurfb.2023.113530.

15. M. Iqbal, A. Yasin, A. Akram, J. A. Li, and K. Zhang, "Advances of Sulfonated Hyaluronic Acid in Biomaterials and Coatings—A Review," *Coatings* 13, no. 8 (2023): 1345, https://doi.org/10.3390/coatings13081345.

16. L. Y. Huang and M. C. Yang, "Surface Immobilization of Chondroitin 6-Sulfate/Heparin Multilayer on Stainless Steel for Developing Drug-Eluting Coronary Stents," *Colloids and Surfaces B: Biointerfaces* 61, no. 1 (2008): 43–52, https://doi.org/10.1016/j.colsurfb.2007.07.004.

17. Y. Hou, X. Zhang, J. Li, L. Wang, and S. Guan, "A Multi-Functional MgF_2/Polydopamine/Hyaluronan-Astaxanthin Coating on the Biodegradable ZE21B Alloy With Better Corrosion Resistance and Biocompatibility for Cardiovascular Application," *Journal of Magnesium and Alloys* 12, no. 3 (2024): 1102–1116, https://doi.org/10.1016/j.jma.2022.06.008.

18. A. Yasin, Y. Ren, J. Li, Y. Sheng, C. Cao, and K. Zhang, "Advances in Hyaluronic Acid for Biomedical Application," *Frontiers in Bioengineering and Biotechnology* 10 (2022): 910290, https://doi.org/10.3389/fbioe.2022.910290.

19. W. Li, L. Ji, J. Tian, et al., "Ophiopogonin D Alleviates Diabetic Myocardial Injuries by Regulating Mitochondrial Dynamics," *Journal of Ethnopharmacology* 271 (2021): 113853, https://doi.org/10.1016/j.jep.2021.113853.

20. K. Zhang, X. Wang, F. Guan, Q. Li, and J. Li, "Immobilization of Ophiopogonin D on Stainless Steel Surfaces for Improving Surface Endothelialization," *RSC Advances* 6, no. 115 (2016): 113893–113898, https://doi.org/10.1039/c6ra17584h.

21. J. Li, W. Li, D. Zou, et al., "Comparison of Conjugating Chondroitin Sulfate A and B on Amine-Rich Surface: For Deeper Understanding on Directing Cardiovascular Cells Fate," *Composites Part B: Engineering* 228 (2022): 109430, https://doi.org/10.1016/j.compositesb.2021.109430.

22. Y. Yu, S. J. Zhu, H. T. Dong, X. Q. Zhang, J. A. Li, and S. K. Guan, "A Novel MgF_2/PDA/S-HA Coating on the Biodegradable ZE21B Alloy for Better Multi-Functions on Cardiovascular Application," *Journal of Magnesium and Alloys* 11, no. 2 (2023): 480–492, https://doi.org/10.1016/j.jma.2021.06.015.

23. J. Li, F. Wu, K. Zhang, et al., "Controlling Molecular Weight of Hyaluronic Acid Conjugated on Amine-Rich Surface: Toward Better Multifunctional Biomaterials for Cardiovascular Implants," *ACS Applied Materials & Interfaces* 9, no. 36 (2017): 30343–30358, https://doi.org/10.1021/acsami.7b07444.

24. J. K. Li, J. J. Su, J. H. Liang, et al., "A Hyaluronic Acid/Chitosan Composite Functionalized Hydrogel Based on Enzyme-Catalyzed and Schiff Base Reaction for Promoting Wound Healing," *International Journal of Biological Macromolecules* 255 (2024): 128284, https://doi.org/10.1016/j.ijbiomac.2023.128284.

25. X. Sun, H. Li, L. Qi, et al., "Construction and Biocompatibility Evaluation of MOF/S-HA Composite Coating on the Surface of Magnesium Alloy Vascular Stent," *Progress in Organic Coatings* 187 (2024): 108177, https://doi.org/10.1016/j.porgcoat.2023.108177.

26. F. Wu, J. Xu, Z. Wang, et al., "Functional Liquid-Infused PDMS Sponge-Based Catheter With Antithrombosis, Antibacteria, and Anti-Inflammatory Properties," *Colloids and Surfaces B: Biointerfaces* 224 (2023): 113208, https://doi.org/10.1016/j.colsurfb.2023.113208.

27. L. J. Qi, Z. Q. Zhang, M. Iqbal, F. Wang, J. A. Li, and S. K. Guan, "Spraying-Assisted Layer-By-Layer Assembled Coatings With Dual Self-Healing Ability to Resist Degradation and Enhance Endothelialization of ZE21B Alloys for Vascular Stents," *Rare Metals* 44, no. 5 (2025): 3405–3427, https://doi.org/10.1007/s12598-024-03159-w.

28. Y. Hou, J. Li, C. Cao, et al., "Biodegradable Mg Alloy Modified With Bioactive Exosomes for Cardiovascular Stent Application," *Journal of Magnesium and Alloys* 12, no. 12 (2024): 4988–5004, https://doi.org/10.1016/j.jma.2023.05.007.

29. Y. Sheng, W. Li, Y. Chai, S. Yin, J. Li, and S. Guan, "A Compound Schiff Base Coating on Biomedical Magnesium Alloy for Enhanced Corrosion Resistance and Biocompatibility," *Smart Materials in Manufacturing* 1 (2023): 100003, https://doi.org/10.1016/j.smmf.2022.100003.

30. F. Wang, Q. Zhao, L. Qi, Y. Hou, J. Li, and S. Guan, "Study on M2-type Macrophage Exosomes Coated With S-HA to Modify Magnesium Alloy Surface for Vascular Scaffolds," *Journal of Magnesium and Alloys* (2025), https://doi.org/10.1016/j.jma.2025.05.011.

31. B. Cai, J. Fang, S. Zhou, et al., "Enzyme-Crosslinked Hyaluronic Acid Hydrogel Scaffolds for BMSCs Microenvironment and Wound Healing," *International Journal of Biological Macromolecules* 295 (2025): 139566, https://doi.org/10.1016/j.ijbiomac.2025.139566.

32. W. Zhang, L. Cui, C. Xie, et al., "Glycocalyx-Inspired Dynamic Antifouling Surfaces for Temporary Intravascular Devices," *Biomaterials* 304 (2024): 122427, https://doi.org/10.1016/j.biomaterials.2023.122427.

33. Z. Xue, X. Sun, H. Li, et al., "Response of Cardiovascular Environment to Sulfonated Hyaluronic Acid With Higher Sulfur Content," *Colloids and Surfaces B: Biointerfaces* 222 (2023): 113046, https://doi.org/10.1016/j.colsurfb.2022.113046.

34. H. Li, F. Wang, X. Sun, et al., "Bio-Inspired Barnacle Cement Coating of Biodegradable Magnesium Alloy for Cerebrovascular Application," *Rare Metals* 43, no. 10 (2024): 10–5185, https://doi.org/10.1007/s12598-024-02794-7.

35. Y. Yang, P. Qi, Y. Ding, et al., "A Biocompatible and Functional Adhesive Amine-Rich Coating Based on Dopamine Polymerization," *Journal of Materials Chemistry B* 3, no. 1 (2015): 72–81, https://doi.org/10.1039/c4tb01236d.

36. N. M. Keeling, M. Wallisch, J. Johnson, et al., "Pharmacologic Targeting of Coagulation Factors XII and XI by Monoclonal Antibodies Reduces Thrombosis in Nitinol Stents Under Flow," *Journal of Thrombosis and Haemostasis* 22, no. 5 (2024): 1433–1446, https://doi.org/10.1016/j.jtha.2024.01.023.

37. Y. Du, X. X. Xu, S. X. Yu, et al., "Dynamics of Endothelial Cells Migration in Nature-Mimicking Blood Vessels," *Talanta* 277 (2024): 126415, https://doi.org/10.1016/j.talanta.2024.126415.

38. L. Wen, H. Qiu, S. Li, et al., "Vascular Stent With Immobilized Anti-Inflammatory Chemerin 15 Peptides Mitigates Neointimal Hyperplasia and Accelerates Vascular Healing," *Acta Biomaterialia* 179 (2024): 371–384, https://doi.org/10.1016/j.actbio.2024.02.022.

39. Y. Cui, X. Jiang, M. Yang, et al., "SEMA4D/VEGF Surface Enhances Endothelialization by Diminished-Glycolysis-Mediated M2-Like Macrophage Polarization," *Materials Today Bio* 23 (2023): 100832, https://doi.org/10.1016/j.mtbio.2023.100832.

40. Z. Zhang, H. Li, T. Min, et al., "Bio-Inspired Barnacle Cement Nano-Composite Coating on Biodegradable Magnesium Alloy for Cerebrovascular Application," *Science China Materials* 69, no. 2 (2025): 1113–1125, https://doi.org/10.1007/s40843-025-3586-7.

41. D. Qiu, J. Yin, Y. Wen, et al., "Diabetes-Induced Iron Stent Degradation but Preventing Re-Endothelialization After Implantation,"

Materials & Design 229 (2023): 111930, https://doi.org/10.1016/j.matdes.2023.111930.

42. S. Park, H. Lee, H. E. Kim, H. D. Jung, and T. S. Jang, "Bifunctional Poly (l-Lactic Acid)/Hydrophobic Silica Nanocomposite Layer Coated on Magnesium Stents for Enhancing Corrosion Resistance and Endothelial Cell Responses," *Materials Science and Engineering: C* 127 (2021): 112239, https://doi.org/10.1016/j.msec.2021.112239.